

Volume 54		Number 8		August 2007		ISSN 0967-0637	
		DEEP-SEA RESEARCH					
Editor: Michael P. Bacon Woods Hole, MA USA		PART I					
Oceanographic Research Papers							
G. BJÖRK, M. JAKOBSSON, B. RUDELS, J.H. SWIFT, L. ANDERSON, D.A. DARBY, J. BACKMAN, B. COAKLEY, P. WINSOR, L. POLYAK and M. EDWARDS		1197	Bathymetry and deep-water exchange across the central Lomonosov Ridge at 88–89°N				
M. MAGAGNINI, C. CORINALDESI, L.S. MONTICELLI, E. DE DOMENICO and R. DANOVARO		1209	Viral abundance and distribution in mesopelagic and bathypelagic waters of the Mediterranean Sea				
S. SHEPHARD, C. TRUEMAN, R. RICKABY and E. ROGAN		1221	Juvenile life history of NE Atlantic orange roughy from otolith stable isotopes				
M.F. VARDARO, D. PARMLEY and K.L. SMITH JR.		1231	A study of possible "reef effects" caused by a long-term time-lapse camera in the deep North Pacific				
D.A. OSBORN, M.W. SILVER, C.G. CASTRO, S.M. BROS and F.P. CHAVEZ		1241	The habitat of mesopelagic scyphomedusae in Monterey Bay, California				
K. FAHL and E.-M. NÖTHIG		1256	Lithogenic and biogenic particle fluxes on the Lomonosov Ridge (central Arctic Ocean) and their relevance for sediment accumulation: Vertical vs. lateral transport				
T.A. VILLAREAL, R.M.L. MCKAY, M.M.D. AL-RSHADAT, R. BOYANAPALLI and R.M. SHERRELL		1273	Compositional and fluorescence characteristics of the giant diatom <i>Ethmodiscus</i> along a 3000 km transect (28°N) in the central North Pacific gyre				
P. MASOUE, J.K. COCHRAN, D.J. HIRSCHBERG, D. DETHLEFF, D. HEBBELN, A. WINKLER and S. PFIRMAN		1289	Radionuclides in Arctic sea ice: Tracers of sources, fates and ice transit time scales				
N. AGARWAL, R. SHARMA, S.K. BASU, A. SARKAR and V.K. AGARWAL		1311	Evaluation of relative performance of QuikSCAT and NCEP re-analysis winds through simulations by an OGCM				
R.E. ROMAN and J.R.E. LUTJEGHARMS		1329	Red Sea Intermediate Water at the Agulhas Current termination				
J.W. MOFFETT, T.J. GOEPFERT and S.W.A. NAQVI		1341	Reduced iron associated with secondary nitrite maxima in the Arabian Sea				
<small>(Contents continued on outside back cover)</small>							
www.elsevier.com/locate/dsr							

This article was published in an Elsevier journal. The attached copy is furnished to the author for non-commercial research and education use, including for instruction at the author's institution, sharing with colleagues and providing to institution administration.

Other uses, including reproduction and distribution, or selling or licensing copies, or posting to personal, institutional or third party websites are prohibited.

In most cases authors are permitted to post their version of the article (e.g. in Word or Tex form) to their personal website or institutional repository. Authors requiring further information regarding Elsevier's archiving and manuscript policies are encouraged to visit:

<http://www.elsevier.com/copyright>



Bathymetry and deep-water exchange across the central Lomonosov Ridge at 88–89°N

Göran Björk^{a,*}, Martin Jakobsson^b, Bert Rudels^c, James H. Swift^d, Leif Anderson^e,
Dennis A. Darby^f, Jan Backman^b, Bernard Coakley^g, Peter Winsor^h,
Leonid Polyakⁱ, Margo Edwards^j

^aGöteborg University, Earth Sciences Center, Box 460, SE-405 30 Göteborg, Sweden

^bDepartment of Geology and Geochemistry, Stockholm University, Stockholm, Sweden

^cFinnish Institute for Marine Research, Helsinki, Finland

^dScripps Institution of Oceanography, University of California San Diego, La Jolla, CA, USA

^eDepartment of Chemistry, Göteborg University, Göteborg, Sweden

^fDepartment of Ocean, Earth, & Atmospheric Sciences, Old Dominion University, Norfolk, USA

^gDepartment of Geology and Geophysics, University of Alaska, Fairbanks, USA

^hPhysical Oceanography Department, Woods Hole Oceanographic Institution, Woods Hole, MA, USA

ⁱByrd Polar Research Center, Ohio State University, Columbus, OH, USA

^jHawaii Institute of Geophysics and Planetology, University of Hawaii, HI, USA

Received 23 October 2006; received in revised form 9 May 2007; accepted 18 May 2007

Available online 2 June 2007

Abstract

Seafloor mapping of the central Lomonosov Ridge using a multibeam echo-sounder during the Beringia/Healy–Oden Trans-Arctic Expedition (HOTRAX) 2005 shows that a channel across the ridge has a substantially shallower sill depth than the ~2500 m indicated in present bathymetric maps. The multibeam survey along the ridge crest shows a maximum sill depth of about 1870 m. A previously hypothesized exchange of deep water from the Amundsen Basin to the Makarov Basin in this area is not confirmed. On the contrary, evidence of a deep-water flow from the Makarov to the Amundsen Basin was observed, indicating the existence of a new pathway for Canadian Basin Deep Water toward the Atlantic Ocean. Sediment data show extensive current activity along the ridge crest and along the rim of a local Intra Basin within the ridge structure.

© 2007 Elsevier Ltd. All rights reserved.

Keywords: Arctic Ocean; Lomonosov Ridge; Bathymetry; Sediments; Deep water; Overflow

1. Introduction

The most striking deep-sea ridge in the Arctic Ocean is the Lomonosov Ridge stretching between

the continental margin of Northern Greenland to the Laptev Sea shelf-off the New Siberian Islands. It rises steeply up to a depth of typically 1000–1300 m below sea level from the 3900–4200 m deep basins on each side and, to the extent that it is unbroken, therefore blocks any direct exchanges of deep water. The Lomonosov Ridge divides the Arctic Ocean

*Corresponding author. Tel.: +46 31 7862858.

E-mail address: gobj@oce.gu.se (G. Björk).

into the two major deep basins: the Eurasian Basin and the Amerasian Basin. The ridge has a clear effect on the deep-water properties, noticeable as a difference in salinity and temperature across the ridge with warmer, saltier and less dense deep water in the Amerasian Basin than in the Eurasian Basin (Worthington, 1953; Aagaard, 1981). These two major deep basins are each sub-divided by distinct deep-sea ridge systems, which also have a significant effect on the deep-ocean properties. The Alpha–Mendeleev Ridge divides the Amerasian Basin into the Makarov Basin and Canada Basin, while the Gakkel Ridge divides the Eurasian Basin into the Amundsen Basin and Nansen Basin (Fig. 1).

Note that the Amerasian Basin is commonly called “Canadian Basin” in oceanographic literature but “Amerasian Basin” is used henceforth in accordance with the geological terminology. When

it comes to description of water masses, we use the generally accepted term “Canadian Basin Deep Water” (CBDP) to specify the deep-water mass in the Amerasian Basin.

The deep and bottom waters of the Makarov Basin are slightly colder and less saline than those of the Canada Basin, and it has been argued that a deep overflow of comparatively fresh and cold deep water from the Amundsen Basin to the Makarov Basin occurs across the central parts of the Lomonosov Ridge (Jones et al., 1995). The density of the water below 1800 m is higher in the Amundsen Basin than in the Makarov Basin, so there is also a potential for a continuous hydraulic flow (Timmermans et al., 2005). A possible location for such overflow is found on the central Lomonosov Ridge at about 88°25′N, 150°E, where the International Bathymetric Chart of the Arctic Ocean (IBCAO) (Jakobsson et al., 2000) shows a channel with sill depth of about 2500 m. This apparent channel was in turn inferred in IBCAO from the Russian bathymetric contour map published in 1999 (Head Department of Navigation and Hydrography, 1999). Because the bathymetric source data of the Russian contour map are classified, it has not been possible for the scientific community to verify the existence of this feature on the central Lomonosov Ridge.

A dedicated field survey of the central Lomonosov Ridge including detailed multibeam bathymetric mapping, subbottom profiling, sediment coring and hydrographic sampling was made during the Beringia/HOTRAX 2005 expedition. The purposes of the survey were to map the seafloor morphology in a sector of the Lomonosov Ridge where overflow of deep bottom waters has been previously hypothesized to occur, and to collect sediment cores and hydrographic data in order to determine whether or not such deep-water overflow takes place. In addition to the new field data collected during the Beringia/HOTRAX 2005 expedition, we have made use of the extensive bathymetric and subbottom-profiling data collected over the Lomonosov Ridge during the SCICEX 1999 expedition with nuclear submarine USS *Hawkbill* (Edwards and Coakley, 2003). Here we present a new digital bathymetric model (DBM) of the central Lomonosov Ridge based on all available depth data together with oceanographic observations that reveal new insights about the exchange of deep waters between the Amerasian and Eurasian Basins.

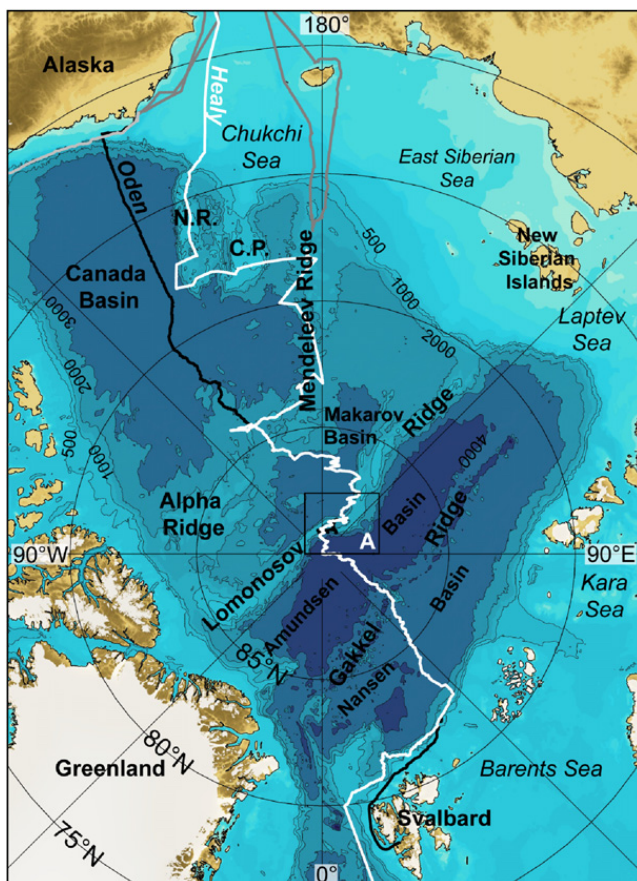


Fig. 1. Bathymetry of the Arctic Ocean with the tracks of icebreaker *Oden* (leg 1: light gray; leg 2: darker gray; leg 3: black) and USCGC *Healy* (white). The box marked A outlines the detailed maps shown in Figs. 2 and 3. N.R., Northwind Ridge; C.P., Chukchi Plateau.

2. Observations and methods

The survey described in this paper was carried out during the summer of 2005 during an expedition across the Arctic Ocean. It was conducted as a two-ship operation between *Oden* and USCGC *Healy*: the Healy–Oden Trans-Arctic Expedition (HOTRAX 2005) (Fig. 1). The work on *Oden* concentrated on physical oceanography and marine chemistry, while *Healy* hosted sediment coring, bathymetric mapping and seismic reflection profiling (Darby et al., 2005). The two ships worked independently until a rendezvous location over the Alpha Ridge at 150°40'W 84°10'N (Fig. 1). Heavy multi-year ice north of the rendezvous point forced both ships toward the west, away from the planned transect across the central Makarov Basin and precluded much of the planned hydrographic sampling and coring program in the Nansen Basin. However, the occurrence of poorly developed lead systems, within a >9/10 overall ice concentration, permitted the target area on the Lomonosov Ridge to be surveyed, albeit with the leads by-and-large dictating the paths of the survey lines.

2.1. Multibeam bathymetry and chirp sonar subbottom profiling

USCGC *Healy* is equipped with a 12-kHz Seabeam 2112 multibeam bathymetric sonar. It has 151 beams and produces a swath of about 2.5–3.5 times the water depth. Multibeam bathymetry was collected continuously with minor interruptions, although the ice conditions greatly affected the quality of the acquired bathymetric data. Sound-speed profiles of the water column for system calibration were acquired at least once a day using the ship's CTD (Sea-Bird SBE 9 Plus), XBTs (Sippican XBT-5 and Sparton XBT-7) or XCTDs (Tsurumi-Seiki's XCTD-1). The bathymetric data were post-processed onboard (cleaned from outliers and gridded) directly after acquisition. The depth measurements derived from the USCGC *Healy* multibeam system is estimated to have an accuracy of $\pm 1\%$ of the water depth or better.

In addition to a multibeam system, the *Healy* has a Knudsen 320B/R dual frequency chirp sonar subbottom profiler (center frequencies ~ 3.5 and 12 kHz). Matched filtered correlated subbottom signals, referred to as “correlates”, were derived through common chirp sonar signal processing techniques (see e.g. Schock et al., 1989) in the

acquisition software and stored in SEG-Y format as well as in Knudsen's native format. The SEG-Y files were post-processed using the public domain seismic software package Sioseis (<http://sioseis.ucsd.edu/>). Envelopes of the subbottom traces (the correlates) were computed through standard signal processing procedures (e.g. Sheriff and Geldart, 1999). Automatic gain control (AGC) was applied when needed, and the subbottom profiles were displayed in gray scales.

2.2. Hydrographic sampling

A Sea-Bird 911 CTD mounted on a 36-bottle rosette sampler was used for the salinity and temperature observations on the *Oden*. The sampling locations were planned to provide information about the deep-water overflow across the Lomonosov Ridge. During operations, it was possible to use the ongoing bathymetric mapping to guide the hydrographic sampling (Fig. 2).

2.3. Sediment coring

Three sites on the Lomonosov Ridge were subjected to sediment coring during the HOTRAX 2005 cruise using a piston and multi-corer (Fig. 2; Table 1). Each multi-corer collects eight 50 cm long tubes, and the sediment surface of these samples is usually undisturbed. For this reason, we have used the multi-corer samples in this study to investigate the seabed physical properties.

2.4. SCICEX bathymetry and subbottom profiles

The SCICEX 1999 submarine expedition with USS *Hawkbill* included a relatively dense survey, ca. 10 km between track lines, of the central Lomonosov Ridge using the Seafloor Characterization and Mapping Pods (SCAMP) (Edwards and Coakley, 2003) (Fig. 2). The SCAMP system contained a sidescan swath bathymetric sonar and a modified Odec Bathy-2000 chirp subbottom profiler (for technical details, see Chayes et al, 1998). The SCICEX swath bathymetry was released for our study as a grid with a resolution of 250×250 m on a polar stereographic projection and the subbottom profiling data as matched filtered correlates stored in SEG-Y format. The SEG-Y files were post-processed applying the same setup as described above for the Knudsen 320B/R data in Sioseis.

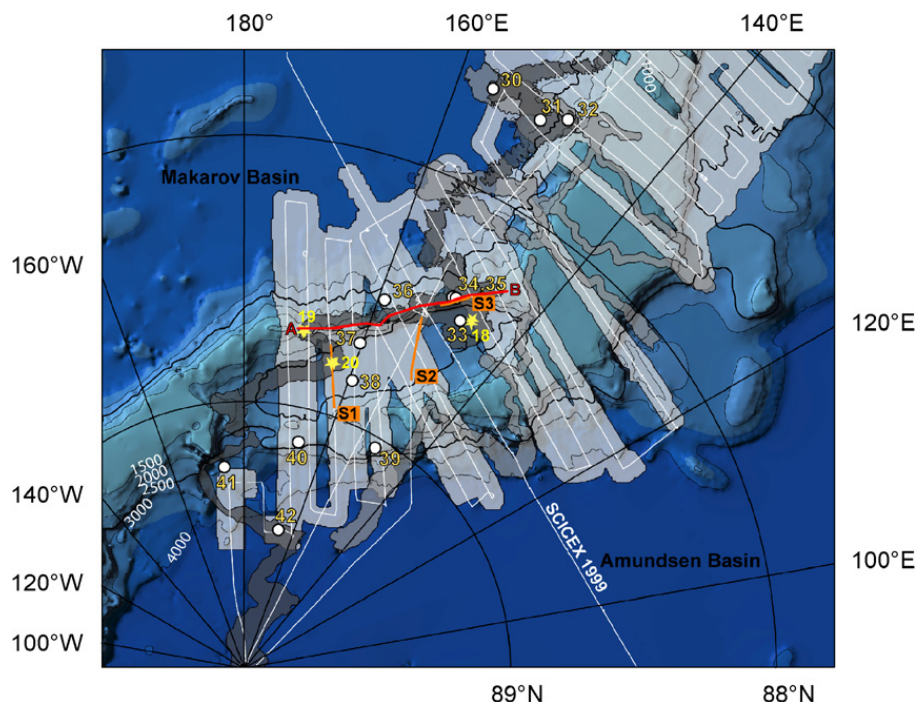


Fig. 2. Map showing bathymetric data sources used to compile a new Digital Bathymetric Model (DBM) with a resolution of 500×500 m on Polar stereographic projection (see text). The bathymetric portrayal underlying the data source information has been based on this new DBM further shown in Fig. 3b. The area filled with light gray shows the coverage of the SCICEX 1999 swath bathymetric data; darker gray shows the multibeam data collected during the R/V *Polarstern* cruise Ark VIII/3 and the darkest gray area represent the coverage of the multibeam data acquired from USCGC *Healy* during the Beringia 2005/HOTRAX expedition. White filled circles show the hydrographic sampling stations carried out from icebreaker *Oden* in 2005, and yellow stars indicate where cores were retrieved from USCGC *Healy*. The red line between A and B is the location of the bathymetric profile shown in Fig. 3c, and the orange lines are the selected SCICEX subbottom profiles shown in Fig. 5a–c.

Table 1
Studied multi-cores

Site (Fig. 2)	Full site name	Latitude (°N)	Longitude (°E)	Depth (m)
18	HLY0503-18MC	88.4371	146.6832	2654
19	HLY0503-19MC	88.7151	169.7856	1023
20	HLY0503-20MC	88.8124	164.0262	2652

Coring site locations are shown in Fig. 2.

2.5. Compilation of the Lomonosov Ridge bathymetry

A DBM was compiled of the Lomonosov Ridge between about $87\text{--}90^\circ$ N and $100^\circ\text{E}\text{--}100^\circ\text{W}$ using all available depth information of the area (Fig. 2). In addition to the multibeam bathymetry acquired during the HOTRAX and SCICEX expeditions, multibeam data acquired during the Ark VIII/3 expedition (Fütterer, 1992) were also used. Furthermore, all single-beam echo soundings contained in the IBCAO database from the area of interest on the central Lomonosov Ridge have been used to

derived the new DBM, which has a grid cell size of 500×500 m on a polar stereographic projection. Bathymetric contours from the Russian map published in 1999 (Head Department of Navigation and Hydrography, 1999) were used only from areas lacking enough direct depth information to derive a 500×500 m resolution DBM. However, it must be emphasized that the area on the Lomonosov Ridge, which is of interest here, is practically fully covered by the HOTRAX, SCICEX and Ark VIII/3 surveys (Fig. 2). In order to interpolate and establish a consistent output between the multibeam, single-beam and contour bathymetric data sets, the

gridding algorithm “surface spline in tension” included in the public domain software generic mapping tools (GMT) (Wessel and Smith, 1991) was applied with the tension parameter set to 0.35. Prior to gridding, the data were block-median filtered using a block size of 500×500 m.

3. Results

3.1. Seafloor morphology

The IBCAO bathymetric portrayal shows that the area between about $88^{\circ}15'–89^{\circ}$ N and $140^{\circ}–180^{\circ}$ E of the Lomonosov Ridge is characterized by a >1000 m deep depression in the ridge morphology forming a local basin, henceforth referred to as the “Intra Basin” (Fig. 3a). Furthermore, IBCAO indicates that the Intra Basin has a sill depth on the Makarov Basin side of about 2500 m, while the sill on the Amundsen Basin side is 2400 m. The critical sill lies between the SCICEX swath lines on the Makarov Basin side at $88^{\circ}25'N$, $150^{\circ}E$ (Fig. 2) and, thus, left it open for speculation whether or not a 2500 m deep passage really exists across the Lomonosov Ridge. To end this uncertainty, the HOTRAX multibeam survey was carried out. The acquired data clearly show that such a deep passage across the ridge does not exist at this location. The Intra Basin sill was mapped to have a maximum depth of about 1870 ± 20 m on the Makarov Basin side (Fig. 3b). The location of this deep(est) passage across the central Lomonosov Ridge, however, is similar to that shown in the previously published IBCAO bathymetry (Fig. 3a and b). A bathymetric profile along the ridge crest on the Makarov Basin side reveals that the ridge here contains at least three pronounced channel-like features including the relatively wide deepest passage and two more narrow passages, of which the deepest reach a depth of about 1670 m (Fig. 4).

The inside walls of the Intra Basin are extremely steep, in particular on the Makarov Basin side, and the basin floor has a water depth generally around 2700 m (Fig. 3b). The floor of the Intra Basin is covered by well-stratified sediments and, south of ca. $88^{\circ}50'N$, it is slightly inclined toward the Makarov Basin wall (Fig. 5a and b). The crossing SCICEX subbottom profiles reveal that the sediment stratigraphy progressively expands toward the deeper parts of the Intra Basin. The part of the profile with the largest layer expansion is close to the Makarov Basin wall in the southern part

(Fig. 5b), whereas the layer expansion occurs in the center of the Intra Basin further toward the Amundsen Basin sill (Fig. 5a). The expanded sections of the stratigraphy are particularly well expressed by two prominent subbottom layers that are acoustically transparent. Moreover, the subbottom profiles along the walls on both sides of the Intra Basin show erosional channels indicative of bottom current activity. Channels are accompanied with occasional acoustically transparent and chaotic sediment depositions that may have resulted from mass wasting from the steep Intra Basin inner slopes (Fig. 5a and b). The channels can be traced in between most of the crossing subbottom profiles, but they could not be mapped by the SCICEX swath bathymetry data which have too coarse a resolution, or by the *Healy* 2005 multibeam data which did not cover the areas where channels are present.

Chirp subbottom profiles acquired during HOTRAX show that the Lomonosov Ridge has been extensively exposed to current activity and erosion on the Makarov flank of the Intra Basin, in particular where the deeper passages exist (Fig. 5c).

In summary, the bottom morphology of the Intra Basin indicates current erosion along the inner walls and sediment deposition in the deeper parts of the basin at locally enhanced sedimentation rates, which is consistent with the expanded stratigraphy.

3.2. Sediment indicators of bottom currents

Studies of the sediment composition of core tops may provide useful information on the existence of bottom currents, although not on the current direction. Of the three cores taken from the Lomonosov Ridge area (Fig. 2), core 19 taken on the Makarov side of the ridge crest contains abundant sand and coarse detritus at the core top, which indicates the influence of bottom currents. Coarse sand and gravel is rare in Holocene sediments in the central Arctic Ocean and concentrations of such suggest current activity that permits only the coarser material to accumulate (Darby et al., 1989, 1997). Because icebergs are rare in the central Arctic Ocean at present, these coarse grains probably derive from fast-ice originating at shorelines (Nürnberg et al., 1994; Reimnitz et al., 1998). Sediment at the top of core 19 also contains manganese micronodules and gravel clasts with manganese coatings, which also suggest very low sedimentation rates (Kennett and Watkins, 1975;

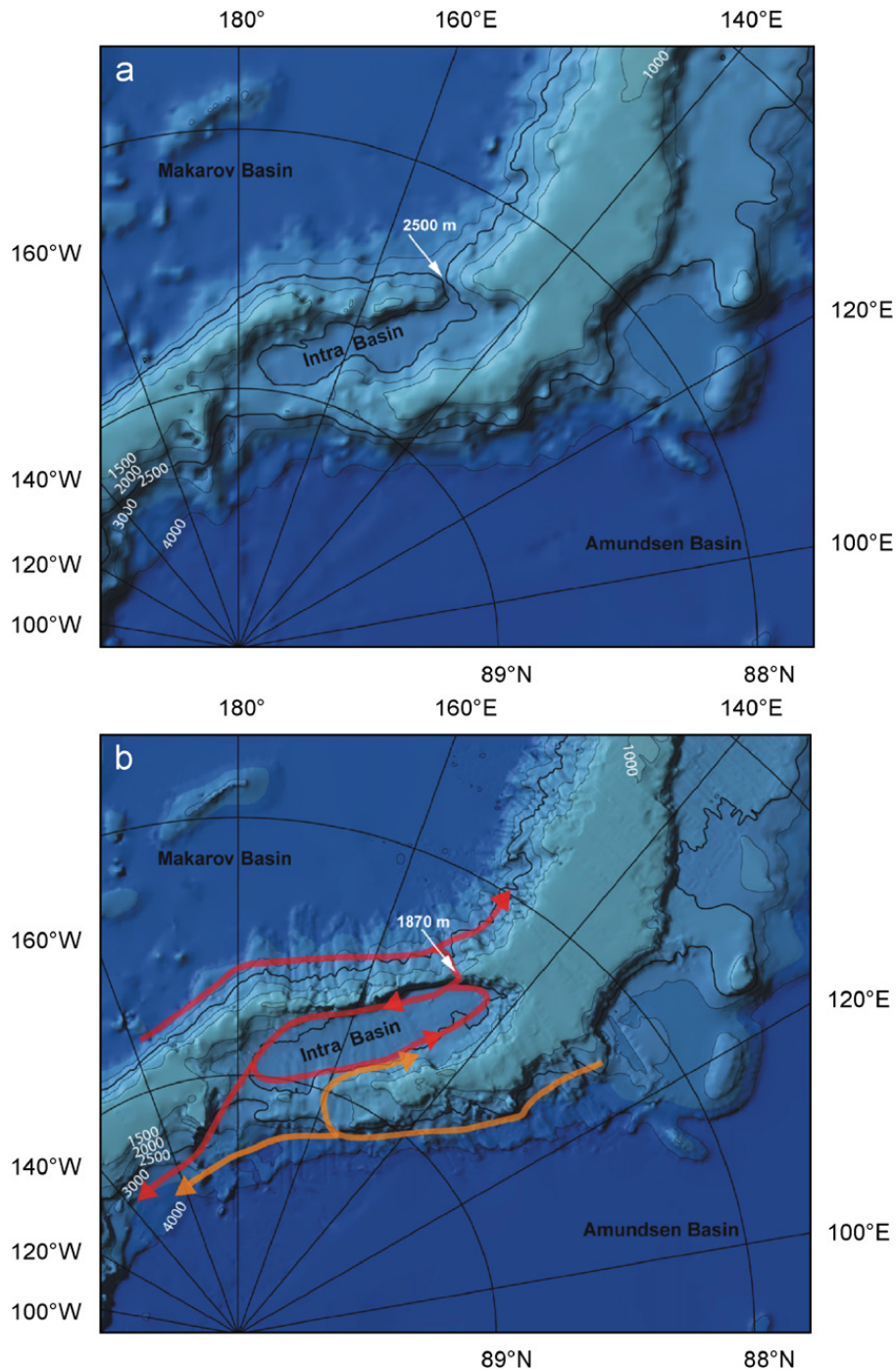


Fig. 3. Comparison between the bathymetry of the central Lomonosov Ridge as portrayed by the 2500×2500 m resolution DBM (a) compiled within the IBCAO project (Jakobsson et al., 2000) and (b) the new 500×500 m resolution DBM compiled here. The bold black contour line shows the 2500 m isobath. Fig. 2 shows the distribution of the bathymetric sources used to assemble the new 500×500 m DBM. Note the large discrepancies between deepest sill depths of the Intra Basin on the Makarov Basin side. Panel (b) includes also the proposed mean circulation of deep waters around the 2000 m level in the Intra Basin area based on hydrographical observations and sediment structures. Red arrows show the flow trajectory of Makarov Basin water and orange arrows the flow trajectory of Amundsen Basin water.

Ledbetter and Watkins, 1978; Post, 1999). Core 20, taken from within the Intra Basin near the wall on the Makarov Basin side (Figs. 2 and 5a), contains some coarse material, but in contrast to core 19

most of this material is biogenic (mollusk shells, tube worms and bryozoans), and manganese coatings occur only on the upper exposed surfaces, suggesting shorter exposure time than at site 19.

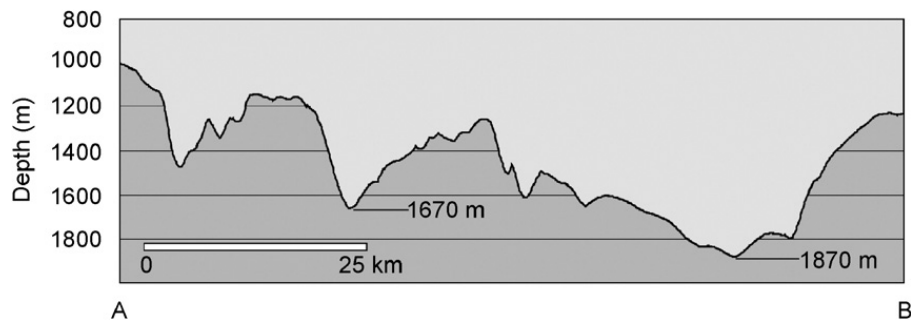


Fig. 4. Bathymetric profile derived from our new DBM along the crest of the Lomonosov Ridge on the Makarov Basin side of the Intra Basin. The exact location of the profile is shown in Fig. 2.

Core 18, retrieved in the Intra Basin away from the steep walls (Fig. 2), does not contain gravel clasts, but only some shell material without coatings, suggesting a quiet depositional environment not affected significantly by bottom currents. Altogether, core-top observations are consistent with subbottom sonar data, both indicating strong current activity at the ridge crest and deposition of fine sediment in the Intra Basin.

3.3. Hydrography

If deep water flows from the Amundsen Basin to the Makarov Basin across the Lomonosov Ridge, one would expect that the overflowing water, after the passage of the sill area, will continue to flow along the ridge slope toward Siberia. The hydrographic stations taken at the Makarov Basin side of the ridge (stations 31 and 32, Fig. 2), downstream (toward Siberia) of the depression, showed however no indications of colder and less saline Amundsen Basin water deeper than 1600 m. Stations 34 and 35, located close to the deepest point found on the ridge crest, indicated the presence of less saline Amundsen Basin water, but this water was not dense enough to sink into the deep Makarov Basin. The bottom-water layer at these stations was distinctly of Makarov Basin origin (see plot of station 35 in Fig. 6). We thus conclude that no significant continuous dense overflow, from the Amundsen Basin to the Makarov Basin, exists in this area. If such overflow exists, it must be either intermittent or located elsewhere.

Stations taken within the Intra Basin (stations 33, 37 and 38) indicate the presence of warm, saline Makarov Basin water between 1700 and 2300 m, having a temperature and salinity maximum at 2000 m (exemplified by station 37 in Fig. 6). The

bottom water in the Intra Basin, was clearly less saline and colder, showing Amundsen Basin water entering across the 2400 m deep sill.

On the Amundsen Basin side of the Lomonosov Ridge, a strong intrusion of warm and saline water was observed between 1700 and 2300 m at station 41, implying an input of Makarov Basin water (Fig. 6). This intrusion was seen on the Greenland side of the Intra Basin while the station taken on the Siberian side of the opening to the Intra Basin (station 39) did not show any presence of Makarov Basin water. This implies that this deep water passes through the Intra Basin and penetrates into the Amundsen Basin between 1700 and 2300 m with its main core around 2000 m, corresponding to the sill depth toward the Makarov Basin. The intrusion of Makarov Basin water was much smaller at station 42, about 25 nautical miles farther into the Amundsen Basin, implying that the inflow originating from the Makarov Basin stays close to the Amundsen flank of the ridge and continues toward Greenland.

The density difference between the two water columns on each side of the Lomonosov Ridge is small above 2000 m, but it increases further down with denser water in the Amundsen Basin (Fig. 6c). The density at sill depth in the Makarov Basin (station 30) is slightly lower, 0.002 kg m^{-3} than at the same level in the Amundsen Basin (stations 40 and 41) (see Fig. 6d). This is too small a difference to force a consistent hydraulic flow in any direction. Compared with density differences for other known overflows such as Gibraltar Strait ($0.85\text{--}1.25 \text{ kg m}^{-3}$), Faroe Bank Channel (0.5 kg m^{-3}) and Denmark Strait (0.38 kg m^{-3}) (Borenäs and Wåhlin, 2000) it is indeed very small. A more likely possibility is that the cross-ridge exchanges occur as disturbances of the main circulation along the ridge. The water mass proper-

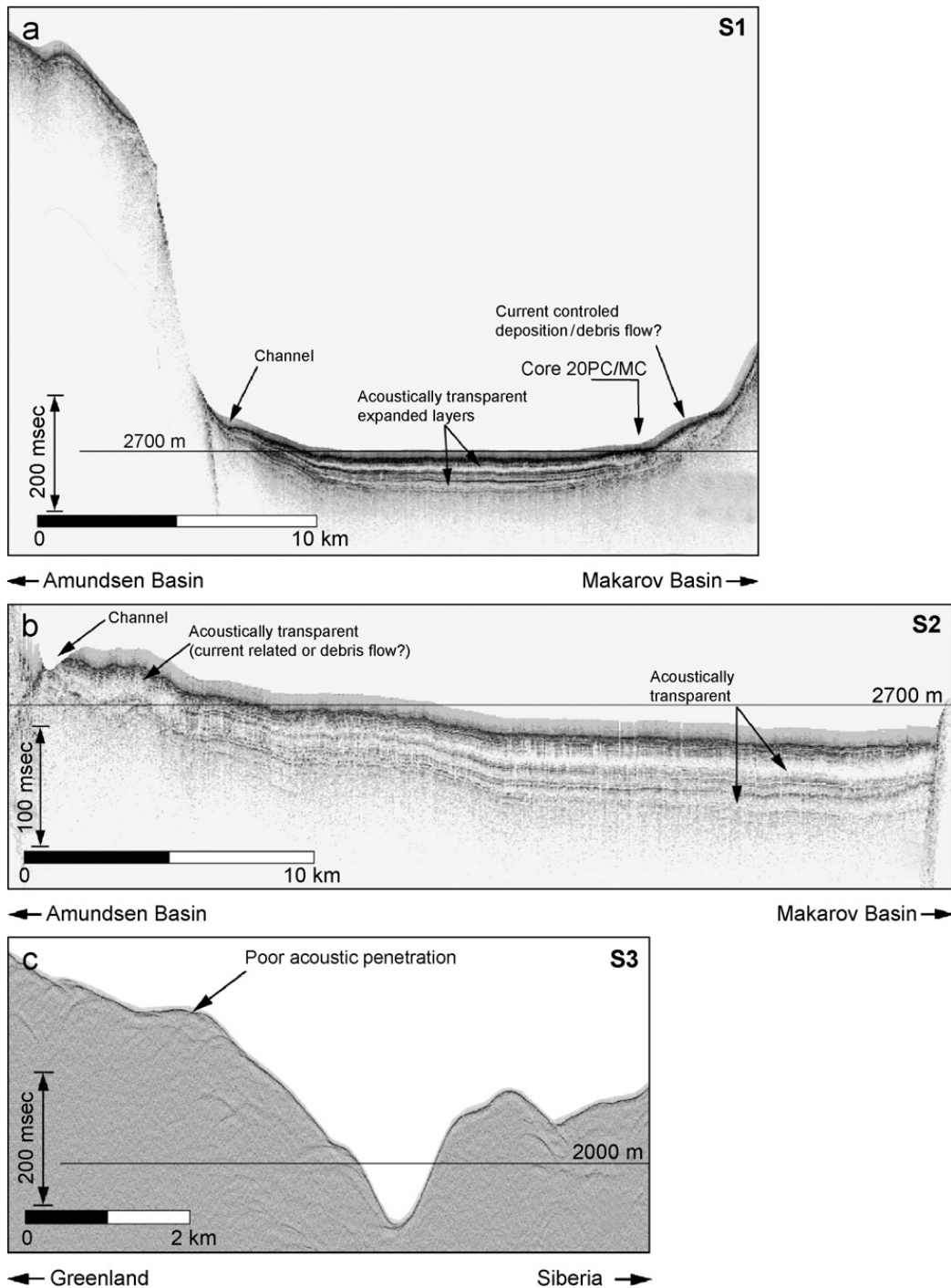


Fig. 5. SCICEX 1999 subbottom profiles S1, S2 and S3 (panels a–c) crossing the Lomonosov Ridge Intra Basin. The locations of these profiles are shown in Fig. 2. Note that profile S3 runs across the deepest channel in the Intra Basin wall, but slightly on the inside, making the channel appear deeper than in the bathymetric profile shown in Fig. 4. 200-ms two-way-travel time equals 150 m for a sediment sound velocity of 1500 m/s and 100 ms corresponds to 75 m.

ties indicate that there is a flow along the Lomonosov Ridge from Siberia toward Greenland on the Amundsen Basin and in the opposite direction on the Makarov Basin side. These flows are mainly barotropic and follow the isobaths. The

main cores of the currents will, however, not be permanently attached to one isobath but will move up and down the slope in response to external disturbances, much-like topographically trapped waves moving along the ridges. This implies that

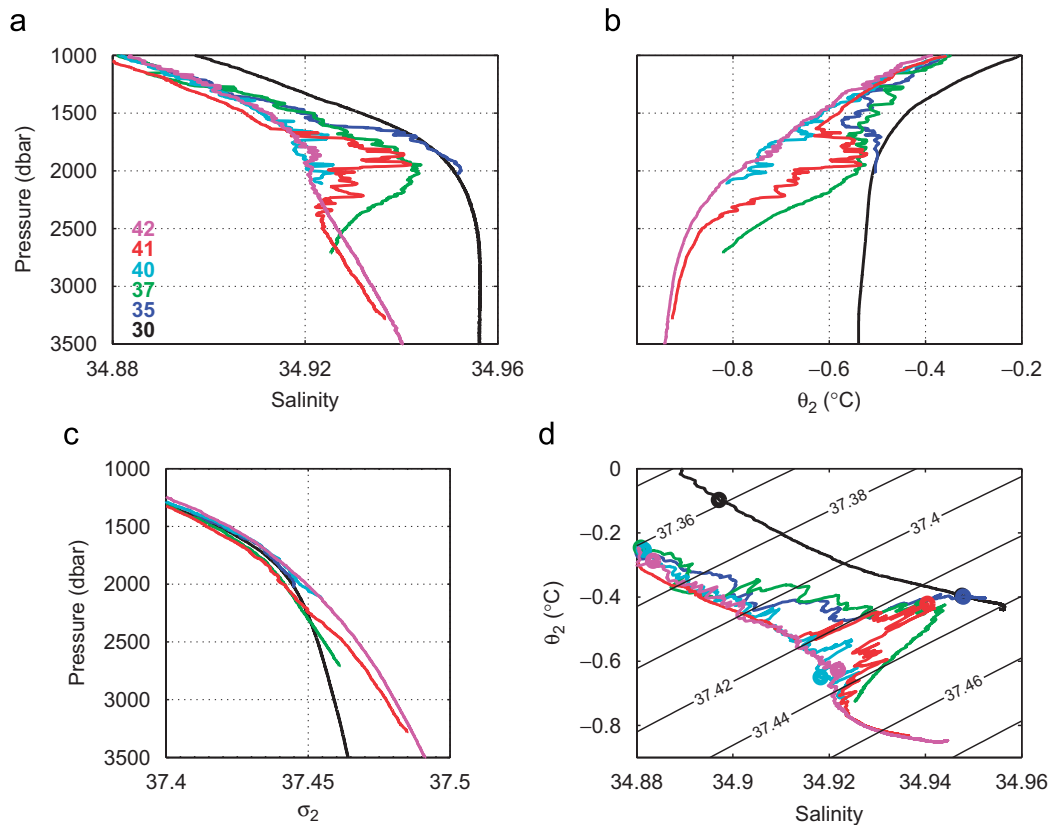


Fig. 6. Salinity profiles (a), potential temperature (θ) profiles (b), potential density (σ_2) profiles referred to 2000 dbar (c) and θ – S curves (d) at the central Lomonosov Ridge. Station 30 is from the Makarov Basin, 35 is located near the sill, 37 from the Intra Basin on the ridge and 40–42 from the Amundsen Basin (see Fig. 2 for positions). The potential temperature (θ_2) and isopycnals are referred to 2000 dbar in the θ – S plot. Filled markers show the 1000 and 1850 dbar levels. The 1850 dbar level is just above the sill depth of the channel.

the main core of the current on the Makarov Basin occasionally will be above, occasionally below the sill depth of the Intra Basin. As it follows the bathymetry it will then either enter or bypass the Intra Basin. Once it has crossed the sill it will follow the slope in the Intra Basin and eventually exit into the Amundsen Basin and continue along the Lomonosov Ridge toward Greenland.

The stratification in the deep Arctic Ocean basins and in the Intra Basin is weak and topographically trapped waves will have large amplitudes. The small bowl-shaped Intra Basin might also sustain other internal wave motions, e.g. Poincaré and Kelvin waves that intensify the vertical motions. Bottom friction will generate a near bottom Ekman transport, which will have a down-slope component for anticlockwise circulation in the Intra Basin and bring some of the Makarov Basin water toward greater depth. It is therefore likely that the signal of the Makarov Basin water will be spread in the vertical as it penetrates into the Intra Basin and into the Amundsen Basin water column. Occasionally

also denser water can be brought over the sill and then sink back to its original level inside the Intra Basin. The Makarov Basin water column in the Intra Basin is thus expected to dominate in a finite depth interval, and the observations indicate that it is spread over about 600 m, from 1700 to 2300 m.

The existence of a sharp front between two, until then, isolated water masses, the deep water from the Makarov Basin and the Amundsen Basin, is a situation highly conducive for creation of interleaving and for double-diffusively driven motions (Rudels et al., 1999). Several maxima and minima in temperature and salinity observed at station 41 indicate that such interaction takes place.

This Makarov Basin water inflow to the Amundsen Basin has not been previously reported, probably because most of the previous crossings of the Lomonosov Ridge were made on the Siberian side of the Intra Basin, upstream of the outflow. This central passage across the Intra Basin thus appears to represent an important pathway for the CBDW toward the Atlantic Ocean. It is observed as

a mid-depth (1700–2000 m) salinity maximum over a large part of the Amundsen Basin (Anderson et al., 1994; Björk and Winsor, 2006), in the Fram Strait (Rudels, 1986), and as a mid-depth temperature maximum in the Greenland Sea (Rudels, 1995).

4. Discussion

The CBDP passes across the central Lomonosov Ridge through the newly mapped Intra Basin between about 88°N and 89°N. This overflow is most probably concentrated in the area where the seafloor topography is characterized by three relatively well-expressed channels in the Intra Basin wall, of which the deepest is 1870 m. Subbottom profiles clearly reveal rough seafloor morphology in the area of these channels, suggesting extensive current activity (Fig. 5c). This conclusion is corroborated by sediment core-top data that shows that the ridge crest is characterized by coarse, manganese-coated debris indicative of bottom current activity, whereas the Intra Basin contains fine sediments deposited in a quiet environment. It should be emphasized that the direction of the water overflow we observe from hydrographic data is opposite to what previously has been proposed (for example see Jones et al., 1995; Timmermans et al., 2005).

Another possible pathway for CBDW across the Lomonosov Ridge is, as suggested by Jones et al. (1995), in a boundary current along the continental slope north of Greenland. There is an approximately 1200 m deep depression between the Lomonosov Ridge and the continental slope of Greenland according to the most recent bathymetric maps (IBCAO: Jakobsson et al., 2000; Head Department of Navigation and Hydrography, 2001), which may guide an overflow in this area. However, the bottom morphology north of Greenland is probably among the least known in the entire Arctic Ocean. The source data used to compile the bathymetric contour maps published by the Russian Head Department of Navigation and Hydrography (1999, 2001) remains classified and, in addition to these published maps, IBCAO has had access only to a few US Navy nuclear submarine tracks from the critical area north of Greenland where the Lomonosov Ridge meets the continental margin. If the sill of this poorly mapped channel is not deeper than 1200 m it cannot provide a direct path for water at the level of the salinity maximum in the Eurasian Basin (1700–2000 m). Still, it cannot yet be

ruled out that overflow of CBDW occurs near Greenland. If this is the case, this water must be denser than the surrounding water masses and sink several hundred meters before it spreads in the Eurasian Basin. There is no observational evidence to indicate that the Amerasian Basin water is significantly denser than the Eurasian Basin water around 1200 m (Timmermans et al., 2005), and it therefore seems unlikely that the source water for the deep salinity maximum in the Eurasian Basin comes from a channel close to Greenland.

The subbottom profiles and the compiled DBM reveal a dynamic environment within the Intra Basin, where bottom-sweeping currents, evident from for example erosional channels, definitely exist (Fig. 5a and b). The Intra Basin has closed depth contours below about 2500 m, giving a possibility for a local gyre circulation. A circulation along closed depth contours may theoretically be forced by the integrated sea surface stress along the contours (Isachsen et al., 2003), but more likely it will be driven by the general circulation along the open and more shallow isobaths. The deep current along the Amundsen Basin flank of the Lomonosov Ridge follows the depth contours and is generally directed toward Greenland according to observations from a current meter mooring relatively close to Siberia (78°30.8'N, 133°57.7'E) placed at 1700 m depth (Woodgate et al., 2001). When this flow reaches the area of the Intra Basin it will be deflected into the basin following the depth contours. It is therefore likely that some Amundsen Basin water will enter the Intra Basin at the northern sill area. The observed flow from the Makarov Basin follows the Makarov Basin flank of the Intra Basin, and these two flows can together set up an overall anticlockwise circulation in the basin. The water mass characteristics around 2000 m in the Intra Basin are consistent with a mixture of Amundsen Basin and Makarov Basin water with a dominance of Makarov Basin water. That mixing occurs in the Intra Basin is also evident from the irregular structure of the temperature and salinity profiles (see Fig. 6) indicating interleaving motions of water with different properties (Rudels et al., 1999). A schematic view of the proposed mean circulation in the Intra Basin and its surroundings is presented in Fig. 3b.

The strength of the circulation in the Intra Basin is likely to be highly variable in response to fluctuations of the large-scale forcing over the Arctic basins and may occasionally be strong

enough to cause erosion of the sediments at the base of the slope within the Intra Basin. Slope currents tend to be strongest where the slope is steep (Isachsen et al., 2003), and it seems plausible that the current at the base of such a steep slope as shown in Fig. 5a and b can give rise to the erosion channels.

Acknowledgments

We are grateful to the Swedish Polar Secretariat for making Oden available for this expedition and for the logistic support. We thank also both captains and the crew on Oden and the US Coast Guard crew on Healy for all their professional support during this challenging expedition. Walter Luis Reynoso-Peralta and Doug White provided valuable assistance in processing the multibeam data during the cruise. Research funds were provided by Swedish Research Council (2004-3958, 2004-5296, 2003-2583, 2005-4727), EU-project CARBOOCEAN (511176-2), Academy of Finland (210651), NSF-OPP 0352395, NSF-0425582, NSF OPP-0425350 and the Swedish Royal Academy through a grant financed by the Knut and Alice Wallenberg foundation.

References

- Aagaard, K., 1981. On the deep circulation in the Arctic Ocean. *Deep Sea Research* 28, 251–268.
- Anderson, L.G., Björk, G., Holby, O., Jones, E.P., Kattner, G., Koltermann, K.P., Liljebladh, B., Lindergren, R., Rudels, B., Swift, J., 1994. Water masses and circulation in the Eurasian basin: results from the Oden 91 expedition. *Journal of Geophysical Research* 99, 3273–3283.
- Björk, G., Winsor, P., 2006. The deep waters of the Eurasian Basin, Arctic Ocean: geothermal heat flow, mixing and renewal. *Deep Sea Research I* 53, 1253–1271.
- Borenäs, K., Wåhlin, A., 2000. Limitations of the streamtube model. *Deep Sea Research I* 47, 1333–1350.
- Chayes, D., Kurras, G., Edwards, M., Anderson, R., Coakley, B., 1998. Swath mapping the Arctic Ocean from US Navy submarines; installation and performance analysis of SCAMP operation during SCICEX 1998. *EOS Transactions of American Geophysical Union* 79 (45), F854.
- Darby, D.A., Naidu, S.A., Mowatt, T.C., Jones, G.A., 1989. Sediment composition and sedimentary processes in the Arctic Ocean. In: Herman, Y. (Ed.), *The Arctic Seas: Climatology, Oceanography, Geology, and Biology*. Van Nostrand Reinhold Co., New York, pp. 657–720.
- Darby, D.A., Bischof, J.F., Jones, G.A., 1997. Radiocarbon chronology of depositional regimes in the western Arctic Ocean. *Deep Sea Research I* 44, 1745–1757.
- Darby, D.A., Jakobsson, M., Polyak, L., 2005. Icebreaker expedition collects key Arctic seafloor and ice data. *EOS* 86 (52), 549–556.
- Edwards, M.H., Coakley, B.J., 2003. SCICEX investigations of the Arctic Ocean system. *Geochemistry* 63 (4), 281–392.
- Fütterer, D.K., 1992. ARCTIC '91: The expedition ARK VIII/3 of RV Polarstern in 1991. *Berichte zur Polarforschung*, no. 107.
- Head Department of Navigation and Oceanography, All-Russian Research Institute for Geology and Mineral Resources of the World Ocean, and Russian Academy of Sciences, 1999. Bottom relief of the Arctic Ocean; map 1:5,000,000. Head Department of Navigation and Oceanography, St. Petersburg, Russia (updated newer version in 2001).
- Isachsen, P.E., LaCasce, L.H., Mauritzen, C., Häkkinen, S., 2003. Wind-driven variability of the large-scale recirculating flow in the Nordic Sea and Arctic Ocean. *Journal of Physical Oceanography* 33, 2534–2550.
- Jakobsson, M., Cherkis, N., Woodward, J., Coakley, B., Macnab, R., 2000. A new grid of Arctic bathymetry: a significant resource for scientists and mapmakers. *EOS Transactions, AGU* 81 (9), 89–93, 96.
- Jones, E.P., Rudels, B., Anderson, L.G., 1995. Deep waters of the Arctic Ocean: origins and circulation. *Deep Sea Research I* 42, 737–760.
- Kennett, J.P., Watkins, N.D., 1975. Deep-sea erosion and manganese nodule development in the southern Indian Ocean. *Science* 188, 1011–1013.
- Ledbetter, M.T., Watkins, N.D., 1978. Separation of primary ice-rafted debris from lag deposits, utilizing manganese micro-nodule accumulation rates in abyssal sediments of the Southern Ocean. *Geological Society of American Bulletin* 89, 1619–1629.
- Nürnberg, D., Wollenburg, I., Dethleff, D., Eichen, H., Kassens, H., Letzig, T., Reimnitz, E., Thiede, J., 1994. Sediments in Arctic sea ice: implications for entrainment, transport, and release. *Marine Geology* 119, 185–214.
- Post, J., 1999. Manganese oxide minerals: crystal structures and economic and environmental significance. *Proceedings of National Academy of Sciences* 96, 3447–3454.
- Reimnitz, E., McCormick, M., Bischof, J., Darby, D., 1998. Comparing sea-ice sediment load with Beaufort Sea shelf deposits: is entrainment selective? *Journal of Sedimentary Research* 68 (5), 777–787.
- Rudels, B., 1986. The theta-S relations in the northern seas: implications for the deep circulation. *Polar Research* 4, 133–159.
- Rudels, B., 1995. The thermohaline circulation in the Arctic Ocean and the Greenland Sea. *Philosophical Transactions of the Royal Society of London* A352, 287–299.
- Rudels, B., Björk, G., Muench, R.D., Schauer, U., 1999. Double-diffusive layering in the Eurasian basin of the Arctic Ocean. *Journal of Marine Systems* 21 (1–4), 3–27.
- Schock, S.G., LeBlanc, L.R., Mayer, L.A., 1989. Chirp subbottom profiler for quantitative sediment analysis. *Geophysics* 54, 445–450.
- Sheriff, R.E., Geldart, L.P., 1999. *Exploration Seismology*, second ed. Cambridge University Press, 592pp. (hardback, 0 521 46826 4 paperback).
- Timmermans, M.-L., Winsor, P., Whitehead, J.A., 2005. Deep-water flow over the Lomonosov Ridge in the Arctic Ocean. *Journal of Physical Oceanography* 35 (8), 1489–1493.

Wessel, P., Smith, W.H.F., 1991. Free software helps map and display data. *EOS Transactions American Geophysical Union* 72 (41), 441, 445–446.

Woodgate, R.A., Aagaard, K., Muench, R.D., Gunn, J., Björk, G., Rudels, B., Roach, A.T., Schauer, U., 2001. The Arctic Ocean boundary current along the Eurasian slope and the

adjacent Lomonosov Ridge: water mass properties, transports and transformation from moored instruments. *Deep Sea Research I* 48, 1757–1792.

Worthington, L.V., 1953. Oceanographic results of Project Skijump I and II in the Polar Sea. 1951–1952. *Transaction of American Geophysical Union* 34 (4), 543–551.